Published in final edited form as:
Circ Res. 2012 July 6; 111(2): 231–244. doi:10.1161/CIRCRESAHA.112.268144.

Molecular imaging of atherosclerosis for improving diagnostic and therapeutic development

Thibaut Quillard, Ph.D. and **Peter Libby, M.D.**
Division of Cardiovascular Medicine, Brigham and Women's Hospital, Harvard Medical School, Boston, Massachusetts 02115, USA

Abstract

Despite recent progress, cardiovascular and allied metabolic disorders remain a worldwide health challenge. We need to identify new targets for therapy, develop new agents for clinical use, and deploy them in a clinically-effective and cost-effective manner. Molecular imaging of atherosclerotic lesions has become a major experimental tool in the last decade, notably by providing a direct gateway to the processes involved in atherogenesis and its complications. This review summarizes the current status of molecular imaging approaches that target the key processes implicated in plaque formation, development, and disruption, and highlights how the refinement and application of such tools might aid the development and evaluation of novel therapeutics.

Keywords

Imaging; Atherosclerosis; Therapeutics development

Introduction

Abundant laboratory and translational evidence has elucidated many mechanisms that contribute to atherosclerosis and its thrombotic complications. Application of such knowledge has already improved outcomes of this disease — notably, the discovery of the low-density lipoprotein (LDL) pathway and the development of statins. Nonetheless, cardiovascular and allied metabolic disorders remain the first cause of death in the United States, and are on the rise worldwide. Mortality data for 2008 show that cardiovascular diseases (CVD) accounted for a third of some 2,500,000 deaths — and associated with an annual cost of almost $300 billion in the United States.[1] We therefore need additional approaches to prevent, detect, and treat coronary atherosclerosis in patients at high risk for clinical events.

Anatomic imaging modalities, such as X-ray contrast angiography, detect coronary stenosis accurately and serve to guide percutaneous and surgical coronary revascularization. This approach can relieve ischemia, but only prevents events or prolongs life in selected subsets of patients. Indeed, autopsy studies indicate that lesions that do not cause a flow-limiting stenosis (<50%) cause most fatal MIs.[2] Thus, we need imaging approaches that reach beyond the visualization of stenosis to develop, validate, and apply novel therapies rapidly

Corresponding Author: Dr. Peter Libby, Division of Cardiovascular Medicine, Department of Medicine, Brigham and Women's Hospital, Harvard Medical School, 77 Avenue Louis Pasteur, Boston, MA 02115; Phone: (617) 525-4383; Fax: (617) 525-4999; plibby@rics.bwh.harvard.edu.

Disclosures
None

and effectively. More recent technologies, like intravascular ultrasonography (IVUS) and carotid ultrasound, have improved the observation of plaques by detecting qualitative differences in plaque composition. But these techniques remain based on contrast analysis, and do not inform specifically on the active cellular and molecular processes that drive the evolution of atherosclerotic lesions.

Molecular imaging has therefore emerged as a novel tool to identify biological aspects of atherosclerotic plaques not captured by anatomical imaging. The refinement and application of such tools could address these needs, not only by improving the detection of lesions, but also by assisting the development and use of therapeutics in preclinical studies and in patients.

Molecular imaging platforms

Molecular imaging relies on various imaging technologies, as reviewed in depth elsewhere.[3] Each approach presents advantages and weaknesses.

X-ray computed tomography (CT) excels for anatomical imaging because of its high spatial resolution and rapidity, but lacks sensitivity and requires exposure to radiation.

Nuclear imaging, including positron emission tomography (PET) and single-photon emission computed tomography (SPECT), provide high sensitivity and allow quantitative measurements, albeit with relatively limited spatial resolution. Moreover, PET/SPECT imaging relies on radioactivity and remains very expensive.

Magnetic resonance imaging (MRI) combines high sensitivity, high spatial and temporal resolution, and functional imaging capabilities. Its limitations include contraindication for certain metallic implants, a restricted array of contrast agents and probes, and cost.

Optical imaging, in contrast, offers high versatility because of its multispectral potential and high resolution. But this modality has low depth penetration of light through tissues, and clinical imaging of deep arteries therefore would require invasive (catheter-based) approaches, currently in development.

Contrast-enhanced ultrasound (CEU) holds promise for molecular imaging because of its relative low cost, wide availability, and high spatial resolution. The challenges of CEU include restricted depth penetration and sensitivity.

Altogether, no current molecular imaging technology by itself is ideal, but co-registration imaging with two or more modalities (e.g., PET/CT, PET/MRI) allows us to combine the benefits of different imaging platforms. For atherosclerosis, researchers and clinicians have developed and tested many imaging strategies that report on the mechanisms involved in plaque formation and destabilization (Table 1). The various imaging approaches described below, by targeting molecular processes involved in various stages of plaque development, also indicate the stage of atherogenesis at a given time point (Figure 2). Sequential imaging sessions afford an opportunity to follow in vivo the evolution of plaques and for assessing the functional impact of therapeutics on atherosclerotic lesions.

Recent advances in atherosclerosis research have revealed new targets for molecular imaging

Low shear stress and Lipid deposition as initiator of the atherogenesis

Recent basic and clinical research has deepened the understanding of molecular and cellular events critical for the pathogenesis of atherosclerosis. First, some regions of arteries show a

particular predisposition to form plaques. Segments that experience low shear stress (LSS) and disturbed flow (e.g., at inner curvatures or bifurcations) show heightened development of early atheromata.[4] Such atherosclerosis-prone regions preferentially accumulate LDL in the subendothelial matrix.[5]

Cell activation

LSS and LDL associate with increased expression of chemotactic molecules (e.g., monocyte chemotactic protein 1 [MCP-1]) and adhesion molecules (vascular cell adhesion molecule 1 [VCAM-1], intercellular adhesion molecule 1 [ICAM-1], E-selectin and P-selectin) that initiate local inflammation. Imaging of cell activation in atherosclerosis development — from early stages to more advanced lesions — currently targets these adhesion molecules overexpressed mainly on endothelial cells (e.g., VCAM-1, ICAM-1, E-selectin, P-selectin).[6, 7] VCAM-1 expressed on activated endothelial cells recruits leukocytes via VLA-4 expressed on leukocytes. Approaches to targeting VCAM-1 have included VLA-4 peptides, anti-VCAM-1 antibody, or a particular peptide of the MHCI molecule that interacts with VCAM-1. Imaging agents link these targeting moieties variously with superparamagnetic iron oxide (SPIO) particles, radionuclides (^{123}I, ^{99m}Tc, ^{18}F), near-infrared fluorescent dyes, or microbubbles for MRI, PET, intravital microscopy (IVM)/ fluorescent molecular tomography (FMT), or CEU. Such targeted nanoparticles accumulate in inflamed cells and tissues in vitro and ex vivo.[8–12] VCAM-1 targeted probes selectively accumulate in mouse atheromata in vivo, and correlate with lipid and VCAM-1 mRNA levels.[13–16] These agents reportedly cause little or no toxicity.[17] ICAM-1-targeted microbubbles can also bind specifically to activated endothelial cells in vitro and to atherosclerotic lesions in carotid arteries in vivo.[18, 19]

To enhance the specific uptake in lesions, combination of targeting moieties for VCAM-1 with E-selectin or P-selectin — also overexpressed on activated endothelial cells — has shown promise in vivo, with a binding over 5-fold more than single targeted MRI probes in vivo.[11, 20] Because activated macrophages can also express VCAM-1 and P-selectin, imaging signals derived from these targeted nanoagents may also reflect indirectly macrophage/foam cell accumulation in the lesions.

Phagocytosis

Expression of adhesion molecules on endothelial cells by LSS and inflammatory signals initiates the recruitment of immune cells to the subendothelial space. In hypercholesterolemic mice, a subset of particularly pro-inflammatory monocytes (Ly6C^{high} CD43^{low}) migrates from its splenic reservoir to nascent lesions.[21] Elevated levels of CD14^{low} CD16^{high} monocytes observed in serum from patients with coronary artery disease (CAD), sepsis, kidney failure, and cancer might correspond to a similar pro-inflammatory monocyte subset in human.[22–25] Cells bearing markers of dendritic cells also accumulate early in such “athero-prone” regions.[26]

Early imaging studies aimed to target these phagocytic cells (mainly macrophages) that rapidly and progressively accumulate in lesions. One of the initial nanoagents developed for imaging used iron oxide particles. Superparamagnetic iron oxide (SPIO, >50 nm) and ultrasmall superparamagnetic iron oxide (USPIO, <50 nm) formulations primarily affect T2 relaxation time for MRI. These nanoparticles consist of an iron oxide crystal core coated with a polysaccharide, synthetic polymer, or monomer. Phagocytic cells take up these nanoparticles spontaneously. In atherosclerotic lesions, the particles rapidly accumulate in macrophages.[27] The SPIO-derived signal correlates well with macrophage load in animal and human atherosclerotic lesions.[28, 29] CD14^{high}CD16^{neg} monocytes displayed a significantly higher SPIO uptake than the CD14^{low}CD16^{high} subset found at a higher

frequency in CAD patients.[25] The phagocytosis of the SPIO agents affected monocyte expression of various markers (CCR2, CX3CR1, MHCII, CD120a, CD206).[30] The ATHEROMA study, which assessed the effects of atorvastatin therapy on reduction of macrophage activity, showed a significant decrease from baseline in USPIO uptake in plaque in the high-dose (80 mg) group after 6 and 12 weeks of treatment.[31] SPIO and USPIO still lack approval by the U.S. Food and Drug Administration (FDA).

In mouse studies, conjugation of these nanoagents with radiolabeled elements (^{64}Cu, ^{18}F) and/or fluorescent dyes allowed multimodal imaging with PET/SPECT and optical imaging of the macrophages in lesions.[32, 33] Combining the high spatial resolution of MRI with the sensitivity and quantification capabilities of PET/SPECT in particular might enhance SPIO's value for atherosclerosis imaging. In addition to MRI, clinical CT can detect macrophage accumulation in plaques, as shown in rabbit atheromata after an injection of iodinated nanoparticles dispersed with surfactant.[34]

Lipids and Oxidatively modified Lipids

When risk factors such as smoking, dyslipidemia, or hypertension overwhelm endogenous protective mechanisms that counter inflammation, macrophages internalize modified LDL (e.g., oxidized LDL [oxLDL]) via scavenger receptors (SRs) including SCR-1, CD36, LOX-1, and other receptors such as TLR2.[35, 36]

At autopsy, large lipid accumulations in lesions (>40%) associate with plaque rupture.[37, 38] Various approaches have targeted lipids or used lipids as a backbone for probes to image atheromata. Examples of such agents include high-density lipoprotein (HDL) and LDL modified with radioisotopes for nuclear imaging (^{123}I, ^{125}I, ^{131}I, ^{111}In, ^{99m}Tc), or chelates for MRI.[39, 40] Patients with clinically symptomatic atherosclerosis took up ^{123}I-LDL in regions of atherosclerosis within 60 minutes.[41]

An alternative approach involves conjugation of imaging agents to ligands that bind lipoprotein receptors. In mice, SR-targeted gadolinium (Gd) particles can provide contrast enhancement of atherosclerosis in vivo, showing correlation between MR enhancement and macrophage content.[42]

CD68 can foster foam-cell formation, as it binds oxidized LDL and mediates its uptake. Administration of an ^{124}I-CD68-Fc imaging probe to apoE$^{-/-}$ mice showed good correlation of signal with the extent of the lesion ex vivo 48 hours after injection.[43] Similarly, PET imaging after injection of ^{99m}Tc-labeled anti-LOX-1 antibody in Watanabe hyperlipidemic rabbits visualized atheromatous lesions, while fibrous plaques yielded less signal.[44] A multimodality probe including MR, PET, and fluorescent tracers with a murine anti-LOX-1 antibody also bound specifically to atherosclerotic plaque in mice.[45] For CEU, microbubbles composed of perfluorocarbon-exposed sonicated dextrose albumin (PESDA) bind to SRs, as confirmed ex vivo by confocal imaging.[46]

Indocyanine green (ICG), an amphiphilic NIR fluorochrome long approved by the FDA for clinical use, binds to LDL and HDL. ICG rapidly binds to lipid-rich inflamed atheroma, in vivo in rabbits and ex vivo in human endarterectomy samples.[47] Imaging of ICG within the coronary artery with a NIRF-sensing intravascular catheter could thus detect lipid-rich lesions.

Metabolic activity

The resultant lipid-engorged macrophages (foam cells) produce pro-inflammatory mediators (e.g., cytokines, chemokines, adhesion molecules) and proteinases (e.g., matrix metalloproteinases [MMPs], cathepsins [Cats], ADAMTS, urokinase [uPA]) that further

sustain the inflammation and accentuate the accumulation of monocytes and vascular smooth-muscle cells (SMCs) in the expanding intima. The SMCs that migrate in the intima lose contractile proteins, but proliferate and secrete more extracellular matrix (ECM) molecules (e.g., collagen). Sites where atheromata develop typically first expand outward due to positive remodeling, thus preventing luminal stenosis detectable by anatomical imaging. The evolving lesion recruits further leukocytes (e.g., more mononuclear phagocytes, T and B lymphocytes, mast cells; in later stages, possibly neutrophils).

Such accumulation of cells in atherosclerotic lesions allows the use of metabolic tracers for imaging. The metabolic activity of macrophages in inflamed lesions, as reflected by uptake of glucose analogs, furnishes an established target for imaging. Cells take up fluorine-labeled 2-deoxy-D-glucose (FDG) at the same rate as glucose. After phosphorylation, FDG accumulates inside the cell. ^{18}F-FDG imaging combines with PET (with its sensitivity and quantitative capabilities) and with co-registered CT for precisely identifying the anatomical source of the PET signal (Figure 1A). This metabolic probe was first used in atherosclerotic patients to assess inflammation and macrophage load in symptomatic carotid artery versus the contralateral asymptomatic control vessel. Higher PET signal in the symptomatic vessel correlated with macrophage staining and expression of inflammatory markers in the retrieved endarterectomy specimen.[48] Dweck et al. reported increased ^{18}F-FDG uptake in the region of the aortic root patients with aortic stenosis, compared to control subjects.[49]

Recent studies report reduced arterial ^{18}F-FDG signal associated with statin treatment, dalcetrapib (an inhibitor of cholesteryl-ester transfer protein, CETP), or lifestyle changes.[50–52] ^{18}F-FDG PET signals in plaques do not correlate closely with anatomical characteristics such as plaque area or plaque thickness. In contrast, FDG uptake does co-localize with macrophages (but not with SMCs) in plaques.[53] We recently demonstrated that hypoxia (another key feature of atherosclerosis), but not exposure to pro-inflammatory cytokines, stimulated FDG uptake in cultured human macrophages.[54] Ogawa et al. also reported that ^{18}F-FDG PET detects the early stage of lipid loading in isolated macrophages, while tracer uptake decreased in fully-formed foam cells in vitro.[55]

In spite of the clinical practicality of ^{18}F-FDG imaging the carotid artery and aorta, monitoring ^{18}F-FDG uptake by lesions in the coronary arteries remains a technical challenge because of the size of the vessel and myocardial uptake. A recent study testing the feasibility of ^{18}F-FDG PET imaging in coronary arteries showed promising results, detecting a stronger FDG-derived signal in the left coronary artery in patients with acute coronary syndrome, compared with stable angina.[56]

Other biotracers in development have less myocardial uptake than FDG. ^{18}F-labeled fluorocholine (FCH) uptake may also reflect metabolic activity. FCH enters a cell via a choline-specific transporter, undergoes phosphorylation by choline kinase, and then is incorporated into the cell membrane. Elevated levels of choline and choline kinase activity in patients with certain cancers spurred the use of FCH. Like tumor cells, macrophages in mouse atherosclerotic lesions can take up FCH ex vivo. Moreover, plaque detection was more sensitive with FCH than with FDG (84% vs 64%).[57] FCH imaging of plaques still requires demonstration in vivo and further mechanistic characterization.

More recently, Camici et al. applied a novel imaging tracer for macrophage activity by radio-labeling a selective ligand of the translocator protein (TSPO) highly expressed by activated macrophages. Symptomatic carotid atheromata showed increased uptake of this probe, compared to asymptomatic plaques. Further ex vivo histological analysis on endarterectomy samples confirmed colocalization of the probe with CD68 (macrophage) staining and its accumulation in macrophage-rich lesions.[58] Clinical exploitation of this

approach still requires validation of the results on a larger population and the use of a more stable radioelement (^{18}F).

Cell death

Lipid–laden foam cells can die, in part due to endoplasmic reticulum (ER) stress. The congregation of lipids and cells in lesions, combined with chronic oxidative stress, local hypoxia, and limited perfusion of nutrients, fosters the formation of a “necrotic,” lipid-rich core within the advancing atheroma.[59]

During apoptosis, activated flippases rapidly redistribute phosphatidylserine (PS) molecules from the inner layer into the outer layer of the cell membrane. Annexin V, a protein that binds to PS, can detect apoptosis.

For atherosclerosis imaging, annexin V has been labeled with radionuclides (^{123}I, ^{124}I, ^{99m}Tc and ^{18}F).[60] In atherosclerotic pigs, SPECT imaging showed a focal accumulation of ^{99m}Tc-annexin-V in the coronary artery in 13 of 22 animals.[61] Atherosclerotic rabbits and mice show similar results, with good correlation between annexin V binding and histological markers of apoptosis.[62] In humans, transplanted hearts undergoing rejection and MI showed increased uptake of these radiotracers.[63] A pilot clinical study tested the predictive value of the uptake of ^{99m}Tc-annexin V on acute vascular events, and showed a specific uptake of the probe in the carotid lesions of two patients who had experienced transient ischemic attacks 3 and 4 days before imaging.[64] Conjugating annexin V with Gd chelates in micelles or to SPIO nanoparticles permitted MR imaging in vivo in the abdominal aorta of atherosclerotic mice. Confocal microscopy further demonstrated association of the probe with macrophages and apoptotic cells in lesions.[65, 66]

Oxidative stress

Oxidative stress observed in lesions may contribute to atherosclerosis by promoting further lipid oxidation and cell death, and by sustaining the inflammatory response.

Antibodies that bind malondialdehyde-lysine (MDA) or oxidized phospholipid epitopes, labeled with radionuclides or conjugated with MR-dedicated micelles, have undergone exploration as imaging agents in experimental atherosclerosis. Aortic uptake of ^{125}I-MDA2 antibody in vivo correlates with lipid-rich plaques and macrophage burden in atherosclerotic rabbits.[67] After 6 months on a low-fat diet, lesions were smaller, with fewer macrophages and more SMCs — features associated with “stable” plaques — and showed ^{125}I-MDA2 uptake.

More recently, probes applicable for MRI (e.g., Gd micelles, USPIO) conjugated to murine and human antibodies against oxidized epitopes (e.g., MDA2, E06, and IK17) showed enhanced magnetic resonance signal in atheromata, compared to adjacent muscle. Confocal imaging confirmed that most of the signal originated from macrophages in lesions.[68]

Reactive oxygen species (ROS) mediate oxidative stress. ROS in atheromata originate predominately from macrophages and SMCs. In particular, plaques contain myeloperoxidase (MPO), an enzyme that generates hypochlorous acid (HOCl/OCl-). MPO can therefore serve as a marker of inflammatory cells and an indirect marker of ROS production. A MR-dedicated probe for MPO (MPO(Gd)) could identify inflammation in rabbit atherosclerotic plaques.[69] A more direct approach targets ROS themselves. Fluorescent nanosensors coated with oxazine fluorophores released by reaction with hypochlorous acid or peroxynitrite (ONOO-) showed a stronger signal in infarcted hearts ex vivo.[70]

Microvessels, neoangiogenesis

When the expanding intima outstrips its oxygen supply, neoangiogenesis can occur. The formation of neovessels in the media and intima derived from the adventitial vasa vasorum often characterize advanced lesions. This neoangiogenesis — while supplying the cells in deep layers of plaques with nutrients and oxygen, therefore potentially preventing cell death — provides an additional gateway for immune cells to inflamed plaques.[71] Moreover, these neovessels tend be fragile and prone to leakage, and can therefore promote intraplaque hemorrhage.

Imaging of the neoformed blood vessels in atherosclerosis profits from the substantial experience collected in cancer research, for which tumor angiogenesis remains a critical diagnostic and therapeutic target. The membranous $\alpha_v\beta_3$ integrin specifically interacts with ECM proteins and soluble ligands, and controls angiogenesis by affecting cell migration, proliferation, and survival.[72] Expression of $\alpha_v\beta_3$ integrin typically associates with neoangiogenic sprouting, and therefore serves as a general marker of angiogenesis. Peptides containing the integrin-binding motif Arg-Gly-Asp (RGD) can image newly formed microvessels. Conjugation of such peptides to Gd-based paramagnetic nanoparticles yielded an increased MRI signal in the abdominal aortic wall of atherosclerotic rabbits.[73] Histological analysis confirmed that the signal derived from the probes correlated with active angiogenesis within the aortic adventitia underlying atherosclerotic plaques. A more recent study in rodents reported similar observations.[74]

Encapsulation of the anti-angiogenic agent fumagillin in these integrin-targeted nanoparticles locally reduced expansion of the vasa vasorum in lesions 1 week following theranostic administration, as observed by MRI and further confirmed by immunohistochemistry (Figure 1B).[75] The combination of an anti-angiogenic drug and atorvastatin synergized and significantly prolonged the efficacy of the treatment, as compared to single-drug controls.[76] Conjugation of RGD peptides to imaging moieties for PET (^{18}F), CEU, and optical imaging (Cy5.5) has efficiently detected plaque burden in atherosclerotic mice and rabbits.[77–79] In mice, uptake of nanoagents in lesions correlated with macrophages — which can also express $\alpha_v\beta_3$ integrin — rather than with neovessel formation that was undetected in the plaques.[77] This observation suggests that these tools could reflect neoangiogenesis, inflammation, or both. Reciprocally, the imaging strategies that target endothelial inflammatory markers like VCAM-1 could also image neoangiogenesis. Indeed, endothelial cells in neovessels overexpress E-selectin and VCAM-1 in response to the inflammatory stimuli released by immune cells within the lesion.[80]

Proteinases

Later in plaque development, the fibrous cap (rich in ECM molecules, notably interstitial collagen), which usually overlies the lipid core, can become thin. In response to inflammatory stimuli, macrophage foam cells produce proteinases that can digest the ECM proteins critical for the lesion’s tensile strength. In particular, elevated MMP collagenase activities cause collagenolysis in the fibrous cap.

More broadly, proteinases (e.g., serine, cysteine, threonine, aspartyl proteinases, and metalloproteinases) affect virtually all aspects of atherosclerotic plaque formation, growth, and complications, in part by degrading extracellular matrix. To image proteinase activity, several groups have employed selective substrates bearing quenched fluorochrome molecules that emit intense fluorescence upon cleavage by the targeted enzyme.

A NIRF-activatable probe detected MMP activity in carotid endarterectomy specimens ex vivo, using either optical imaging or multispectral optoacoustic tomography.[81, 82] In mice,

proof-of-concept studies have imaged gelatinase activity (MMP-2 and MMP-9) in vivo using an activatable NIRF substrate.[83] In experimental MI and atherosclerosis, IVM and FMT showed increased gelatinase activity in macrophage-rich lesions and infarct areas, as confirmed ex vivo by fluorescent reflectance imaging (FRI) and in situ zymography. The use of a comparable MMP probe demonstrated active MMPs in human carotid atheromata ex vivo. More recently, we used a similar approach to assess MMP-13 activity after administrating a selective MMP-13 inhibitor orally to atherosclerotic mice.[84] IVM and ex vivo FRI both reported a marked decrease in NIRF signal derived from a MMP-activatable probe after 10 weeks of treatment (Figure 1C). Others have used a similar approach to show *in vivo* the reduction of MMP activity and macrophage accumulation in plaques following treatment with pioglitazone (PPARγ inhibitor).[85]

Such so-called “smart” probes are also in development for in vivo assessment of cathepsin activity in atherosclerosis. In an early study, FMT co-registered with MRI detected a strong signal in aortic plaques of atherosclerotic mice after injection of a Cy5.5-labeled activatable probe for Cat-B. Histological analysis confirmed a higher expression of Cat-B, which colocalized with macrophage staining.[85] Ex vivo imaging also demonstrated that statin treatment associated with reduced Cat-B activity in lesions.[86] Similarly, IVM and ex vivo FRI following administration of an activatable probe specific for Cat-K revealed more than twice as much signal in atherosclerotic mice and in human carotid endarterectomy specimens, as compared with the control agent.[87]

The lysosomal cysteine proteinase Cat-S colocalizes with regions of plaque calcification, shown by NIRF signals derived from a Cat-S-activatable probe and a fluorescent osteogenesis-targeted agent coinjected in mice with experimentally induced chronic renal disease.[88] With a more clinically relevant approach, a broad cathepsin-activatable probe was injected into atherosclerotic rabbits. NIRF imaging of the iliac artery with an intravascular catheter successfully detected the fluorescent signal in the lesions derived from cathepsin proteolytic activity.[89]

MR-dedicated “smart” probes have also been described for MR and nuclear imaging platforms. MMP-2/MMP-9 substrates conjugated with Gd or iron oxide core nanoparticles, and a substrate for MMP-14 radiolabeled with ^{99m}Tc, are under investigation.[90–92] A synthetic peptide that specifically binds MMPs conjugated with a Gd chelate yielded a two-fold increase in MR image signal intensity of atherosclerotic lesions in vivo in atherosclerotic mice, compared to healthy controls.[93] Confocal microscopy further confirmed the colocalization of agent signal and MMPs (MMP-2, MMP-3, and MMP-9) in lesions, particularly those present in the fibrous cap region. While initially and still evaluated in vitro, in cancer, or in live animals, no study has yet assessed the potential of these agents in CVD in humans.

Another approach to imaging proteinases uses specific or broad-range inhibitors labeled by imaging moieties. Early studies reported the development of MMP inhibitors (MMPIs) coupled with ^{123}I, ^{99m}Tc, and ^{18}F to assess MMP expression in cancer or to screen other MMPIs by SPECT or PET imaging.[94, 95] Later investigations have correlated ^{99m}Tc- or ^{111}In-MMPI signals with macrophages and MMP-2/MMP-9 activity in atheromata and aneurysms by multimodal SPECT/CT imaging.[96, 97] The use of non-substrate ligands for MMPs foregoes the advantage of catalytic activation by the enzymes that can yield a considerable amplification of signal. Dual radionuclide labeling approaches, as used by Haider et al. in 2009, could therefore combine imaging targets to visualize MMP activity (^{99m}Tc-labeled MMPI) and other molecular processes, like cell apoptosis (^{111}In-labeled annexin V), using PET-SPET/CT to characterize features of plaques associated with rupture.[96]

Extracellular matrix (ECM)

Visualization of collagen levels in lesions, and particularly within the fibrous cap, could indicate plaque "stability". Several groups have designed imaging agents dedicated to collagen, for estimating plaque collagen in vivo.[98, 99] These probes combine CNA-35, a collagen adhesion protein of the *Staphylococcus aureus* bacterium, in paramagnetic micelles for MR or with fluorescent dye for optical imaging. Initial studies showed colocalization of the probes injected in vivo, with collagen in lesions ex vivo. Moreover, abdominal aortic aneurysms in mice showed signal enhancement in the region injected with CNA-35 micelles, 36 hours after injection. Postmortem histology attested that the signal derived from the CNA-35 micelles colocalized with collagen-I rich areas in the adventitia.[98]

Two-photon excited fluorescence and second-harmonic generation takes advantage of the intrinsic optical properties of collagen fibers, and allows the detection of collagen with a very high spatial resolution.[100] This modality, which does not require an exogenous probe, remains limited to preclinical research because of its very limited depth of field. An intravascular catheter-based strategy could aid clinical adoption in the future.

Thrombus, intraplaque hemorrhage

When thin and fragile, the fibrous cap can ultimately fracture and expose the pro-thrombotic content of the lesion's core to the circulating coagulation factors. This critical event can trigger thrombosis that can cause clinical events.[101, 102]

During the coagulation cascade, thrombin-mediated cleavage of fibrinogen produces fibrin monomers. The fibrin clot assembly, stabilized by crosslinking via factor XIII, can produce obstructive thrombi. Molecular imaging targeting each of these steps could detect sub-occlusive thrombosis and intraplaque hemorrhages.

One approach to imaging such processes in vivo targets activated platelets via P-selectin or glycoprotein IIb/IIIa (also called integrin $\alpha_{IIb}\beta_{IIIa}$, and referred to as Gp IIb/IIIa). Imaging probes targeting P-selectin through a specific antibody (VH10), interacting peptides, or polysaccharides bind efficiently in vitro and in vivo to platelets and thrombi by SPECT or MRI.[103, 104] The lack of selectivity, however, for platelets in complex, advanced lesions — macrophages and endothelial cells can also express P-selectin — can confound interpretation of whether signal reflects thrombosis, inflammation, or (more likely) both. To detect platelets more selectively, imaging agents for MRI, optical imaging, PET, and CEU targeting glycoprotein IIb/IIIa have emerged in the last few years. Peptides or antibodies that recognize selectively the activated conformation of the protein (anti-ligand–induced binding sites [LIBS]) permit molecular targeting.[105, 106] While most studies have reported in vitro or ex vivo validation of probe selectivity for activated platelets and thrombi, in vivo validation remains scarce.[107]

As fibrin localizes in thrombi, but not in circulating blood, this alternative approach confers a high specificity for thrombus imaging. In particular, EP-2104R consists in a short peptide that binds to fibrin, conjugated with Gd for MRI. Administration of the probe to 52 subjects with suspected thrombotic events showed selectivity for arterial clots (84%) over venous clots (29%).[108] A ^{64}Cu-radiolabeled EP-2104R probe allowed multimodality detection of fibrin deposits within arterial thrombus in rats.[109] Thrombus enhancement occurred in all 5 rats imaged by MR/PET.

An additional approach currently investigated for thrombogenesis imaging targets factor XIII using peptide substrates for factor XIII.[110, 111] These peptide agents are covalently cross-linked into clots actively undergoing thrombogenesis by factor XIII, yielding a time-dependent increase in the fluorescence signal. Such an agent might distinguish acute thrombi

from subacute thrombi in vivo. In these studies, the targeting peptides conjugated on fluorescent SPIO nanoparticles allowed the detection of vascular thrombi in vitro and in vivo in mice, using both NIRF and MR imaging. Similar results occurred in other studies using Gd-based MR agents conjugated to comparable targeting sequences.[112, 113]

Microcalcification

Local calcification in the lesion can also jeopardize plaque stability by increasing stiffness and biomechanical inhomogeneities.[114] Patients with a family history of premature CVD have shown increased arterial calcification,[115] an increased burden of subclinical coronary lesions, and a predilection for coronary heart disease events.[116, 117] Calcification, an active process, involves inflammatory signals that alter local expression of the endogenous activators (e.g., ALK, osteopontin, Runx2/Cbfa1, osteocalcein, members of the Notch family) and inhibitors (e.g., MGP, fetuin, osteoprotegerin) of osteogenesis, and favor the accumulation of lesional calcium.

While CT, IVUS, and MRI can detect advanced bone-like structures without the need for specific molecular probes, we still require additional imaging approaches to detect and quantify early osteogenesis within the vessel wall.

A bisphosphonate-conjugated imaging agent that binds to nanomolar concentrations of calcium hydroxyapatite complexes permits optical imaging for the experimental detection of the early stages of mineralization.[118] Ex vivo analysis colocalized the expression of the key regulators of osteogenesis and osteoblastic cells with fluorescence.[119] This probe permits imaging calcification in early experimental atherosclerosis, and statin therapy reduced osteogenic activity concomitant with decreased inflammatory burden.[120] This result further supports the causal link between inflammation and vascular calcification in atheromata.[121]

PET-CT using fluorine-18-sodium fluoride (^{18}F-NaF) can also image calcification in lesions.[122] The uptake of ^{18}F-NaF relies on the exchange of hydroxyl ions in the hydroxyapatite crystal, an indicator of bone metabolic activity. This approach showed retrospectively in 51 patients that ^{18}F-NaF uptake in the aorta increased significantly with age. Uptake of the tracer in patients presenting with aortic stenosis displayed a progressive increase with the degree of stenosis.[49] While still preliminary, these studies highlight the potential of PET-CT for detection and quantification of early calcification in plaques.

Impact of imaging on monitoring and developing therapies for cardiovascular diseases

Molecular imaging promises to transform the monitoring and development of cardiovascular therapies. The pathway to achieving this promise, however, requires overcoming several barriers. This section will illustrate how molecular imaging could advance cardiovascular therapeutics, and the next section will highlight the challenges.

No one imaging modality will meet all clinical needs optimally. The choice of an imaging approach should reflect the biological processes that represent the most likely or informative aspects of the therapeutic target. Anatomical imaging approaches, for example, can assess plaque volume and help estimate the burden of atherosclerotic disease. Indeed, methodologies such as intravascular ultrasound have proven useful in demonstrating alterations in coronary arterial plaque volume in response to lipid interventions such as LDL lowering or administration of HDL-like preparations.[123–125] Molecular imaging may therefore aid the clinical development of novel approaches to the treatment of dyslipidemia. HDL, for example, beyond a putative role in reverse cholesterol transport, may exert anti-inflammatory and/or antioxidant effects.[126] Molecular imaging approaches that report on

inflammation or oxidative stress should aid the clinical evaluation of therapeutics that will raise HDL. As levels of plasma HDL likely reflect poorly the putative anti-inflammatory and anti-oxidant properties of HDL, molecular imaging strategies might help validate approaches such as CETP inhibitors with different nuances of mechanistic profiles, small molecule HDL mimetics, and variations on apolipoprotein A1 administration.

Likewise, molecular imaging of inflammation — for example, by protease activity, monitoring of phagocytosis, or leukocyte recruitment or accumulation — also may help the development of interventions that target inflammation, small molecules such as methotrexate or other anti-inflammatory drugs, or selective modulators of peroxisome proliferation activation receptors (PPARs).[85, 127]

Several immunomodulatory therapies — both biological and small-molecule — have entered clinical practice. Anti-B-cell monoclonal antibodies, for example, currently have application in oncology and in non-cardiovascular inflammatory diseases.[128–131] Vaccination or passive targeting of LDL or modified LDL are also entering clinical development.[132, 133] Molecular imaging strategies that report on lymphocyte recruitment might provide an approach to monitoring these therapies when applied to atherosclerotic plaques that could prove particularly informative.

Cardiovascular calcification provides another potential novel target for molecular imaging. While monitoring the accumulation of calcium mineral in plaques by established techniques, such as calcium artery scoring or CT angiography, may reflect plaque burden and provide prognostic information, monitoring changes in calcium mineral content has proven disappointing in clinical trials as a biomarker of clinical benefit.[134] Recent advances in understanding the biology of calcification reveal new targets for imaging the biological processes that may precede macro-calcification.[135] Harnessing this novel insight could provide promising targets for novel therapies aimed at modulating calcification.

Barriers to translation of molecular imaging in cardiovascular therapeutics

Molecular imaging, although promising and enticing, faces substantial barriers to achieve clinical utility. Various modalities that can visualize molecular targets have limitations in different arterial beds. For example, currently cardiac and respiratory motion impede the use of MRI in the coronary circulation where plaque rupture may have considerable clinical impact.[136] The development of imaging agents with practicability for clinical translation has begun, but will require considerable further work for optimization. Imaging agents dedicated for intraplaque processes, for example, need to achieve access to advanced human lesions, which presents a greater challenge that required for mouse atheroma. As plaque microvessels may have augmented permeability, they could provide a portal for entry of molecular imaging agents. Also, some current imaging targets lack specificity for specific cell types (e.g. not only endothelial cells, but also smooth muscle cells and macrophages can express VCAM-1). Yet, as inflammatory activation elevates VCAM-1 on all these cell types, agents that target this structure may still reveal a biological process important in lesion progression and complication despite the lack of specificity for only one cell type. Indeed, the expression of VCAM-1 by several relevant cell types may enhance the imaging signal.

Once suitable imaging agents have undergone optimization, obtaining clinical-grade material according to good manufacturing processes (GMP) production represents another barrier. The resources of academic laboratories seldom include access to appropriate facilities for GMP production. Thus, achieving sterile and pyrogen-free materials and ascertaining quality will likely prove impractical for most academic institutions. While the cooperative development of such probes would seem to provide a pre-competitive advantage

to the pharmaceutical industry, appropriate consortia do not yet exist. While governmental support — including the Science Moving towArds Research Translation and Therapy (SMARTT) program from the National Heart, Lung, and Blood Institute — may provide some assistance in this regard, commercial manufacturers of imaging equipment show limited interest and ability to support sustained programs to provide imaging diagnostics. While such products may prove very useful for drug development and research, many concerns view them as having limited commercial potential, particularly in an era when health care reform casts more stringent controls on the clinical use of imaging technologies.

Such clinical-grade material would require extensive toxicologic testing before use in humans. The usual array of toxicologic evaluations extends beyond the reach of most academic laboratories. Some of the same barriers that confront GMP production challenge the evaluation of toxicity required for human use.

Another issue regarding the clinical application of molecular imaging revolves around the translatability of imaging platforms. NIRF signals, for example, permit visualization of deep cardiovascular structures in small animals such as mice. The visualization of deep vessels in humans — the coronary arteries, for example — would require greater tissue penetration than that afforded by NIRF. This approach, while suitable for non-invasive imaging of small animals, would likely require the development of invasive, catheter-based technologies for clinical applicability.[89] Such platforms, currently under development, would also require a thorough safety evaluation to obtain regulatory approval for human application. As both device and laser safety concerns pertain to such catheters, ascertaining safety for regulatory purposes presents another hurdle to the clinical application of this technology.

The potential of molecular imaging to aid the development of novel cardiovascular therapeutics

Despite the barriers outlined above, the successful introduction of molecular imaging in the clinic could make critical contributions to the development and evaluation of novel cardiovascular therapeutic interventions (Figure 2). The ability of molecular imaging to interrogate biological processes rather than anatomical features could provide a new dimension of information in these applications. Molecular imaging might aid the detection of lesions that exhibit features associated with rupture — so-called “vulnerable plaques”. A recent review in this series from our colleagues described the potential diagnostic use of molecular imaging approaches in more detail.[3] Here, we illustrate how molecular imaging could guide the development of therapeutics and assessing the efficacy of treatment (Figure 3). In preclinical development, molecular imaging could serve to validate the effects of interventions on particular targets and enhance the proof of concept of novel therapeutic interventions — notably, pharmacologic agents. Such an approach would verify the targeting of specific biological processes in vivo, complementing results from in vitro screens. The same principle could apply to humans. A crucial quandary for the cardiovascular application of novel therapeutics involves the ability of an agent to act in intact humans on the putative target. Molecular imaging could help bridge the gap between experimental application in animals and humans.

Finally, dose selection provides a considerable challenge to the design of clinical trials. Given the low event rates due to the current standard of care, the size and duration of clinical trials to demonstrate additional benefit over and above existing therapies has grown. The resources required for clinical efficacy trials that measure clinical endpoints have become daunting for these reasons. The ability to refine dose selection for evaluation in clinical endpoint trials by molecular imaging could revolutionize this process. Defining doses for clinical trials currently depends upon extrapolations from animal observations,

pharmacokinetic modeling using informatic approaches, and the use of soluble biomarker data from humans. While soluble biomarkers provide an indirect window on biological processes of interest, they do not provide assurance that an agent achieves sufficient concentration at the site of the targeted pathological process in vivo to exert its effect. Moreover, an appropriately designed molecular imaging strategy could provide early hints of clinical efficacy by showing an effect on the biological process of interest in vivo with a particular dose of an agent. While even imaging biomarkers will likely not suffice for the registration of novel cardiovascular therapeutics in the foreseeable future, the information from imaging signals could provide considerable reassurance regarding the choice of dose and the decision to proceed with a large-scale clinical endpoint trial. This potential of molecular imaging could help to streamline cardiovascular drug development, reduce the risk of embarking on clinical endpoint trials, and ultimately speed the availability of novel therapeutics that can address the residual burden of cardiovascular risk — a major and growing worldwide challenge to human health and quality of life.

Acknowledgments

We thank our colleagues affiliated with the Donald W. Reynolds Clinical Cardiovascular Research Center at Harvard Medical School, who contributed to our efforts to develop molecular imaging of atherosclerosis and cardiovascular diseases. We gratefully acknowledge Marcelo F. Di Carli, M.D. for the ^{18}F-FDG uptake illustration. We also acknowledge the National Institutes of Health (R01-HL080472), and the Translational Program of Excellence in Nanotechnology (TPEN) (U01 HL080731) for their support.

Non-standard Abbreviations and Acronyms

CAD	coronary artery disease
Cat	cathepsin
CETP	cholesteryl-ester transfer protein
CEU	contrast-enhanced ultrasound
CT	computed tomography
CVD	cardiovascular diseases
DCE	dynamic contrast-enhanced
ECM	extracellular matrix
ER	endoplasmic reticulum
FCH	fluorocholine
FDG	fluorine-labeled 2-deoxy-D-glucose
FMT	fluorescent molecular tomography
FRI	fluorescent reflectance imaging
Gd	gadolinium
GMP	good manufacturing processes
HDL	high-density lipoprotein
ICAM-1	intercellular adhesion molecule-1
ICG	indocyanine green
IVM	intravascular microscopy
IVUS	intravascular ultrasonography

LDL	low-density lipoprotein
LIBS	ligand-induced binding sites
LOX-1	lectin-like oxidized low-density lipoprotein receptor 1
LSS	low shear stress
MCP-1	monocyte chemotactic protein-1
MDA	malondialdehyde-lysine
MGP	Matrix Gla protein
MI	myocardial infarct
MMP	matrix metalloproteinase
MMPI	matrix metalloproteinase inhibitor
MPO	myeloperoxidase
MRI	magnetic resonance imaging
NIRF	near-infrared fluorescence
PESDA	perfluorocarbon-exposed sonicated dextrose albumin
PET	positron emission tomography
PPAR	peroxisome proliferator-activated receptor
PS	phosphatidylserine
ROS	reactive oxygen species
SMC	smooth-muscle cell
SPECT	single-photon emission computed tomography
SPIO	superparamagnetic iron oxide
SR	scavenger receptor
TLR	Toll-like receptor
TSPO	translocator protein
USPIO	ultrasmall superparamagnetic iron oxide
VCAM-1	vascular cell adhesion molecule-1

References

1. Roger VL, Go AS, Lloyd-Jones DM, Adams RJ, Berry JD, Brown TM, Carnethon MR, Dai S, de Simone G, Ford ES, Fox CS, Fullerton HJ, Gillespie C, Greenlund KJ, Hailpern SM, Heit JA, Ho PM, Howard VJ, Kissela BM, Kittner SJ, Lackland DT, Lichtman JH, Lisabeth LD, Makuc DM, Marcus GM, Marelli A, Matchar DB, McDermott MM, Meigs JB, Moy CS, Mozaffarian D, Mussolino ME, Nichol G, Paynter NP, Rosamond WD, Sorlie PD, Stafford RS, Turan TN, Turner MB, Wong ND, Wylie-Rosett J. Heart disease and stroke statistics--2011 update: A report from the american heart association. Circulation. 2011; 123:e18–e209. [PubMed: 21160056]
2. Virmani R, Burke AP, Farb A, Kolodgie FD. Pathology of the vulnerable plaque. J Am Coll Cardiol. 2006; 47:C13–18. [PubMed: 16631505]
3. Leuschner F, Nahrendorf M. Molecular imaging of coronary atherosclerosis and myocardial infarction: Considerations for the bench and perspectives for the clinic. Circ Res. 2011; 108:593–606. [PubMed: 21372291]

4. Chiu JJ, Chien S. Effects of disturbed flow on vascular endothelium: Pathophysiological basis and clinical perspectives. Physiol Rev. 2011; 91:327–387. [PubMed: 21248169]
5. Miyazaki T, Taketomi Y, Takimoto M, Lei XF, Arita S, Kim-Kaneyama JR, Arata S, Ohata H, Ota H, Murakami M, Miyazaki A. M-calpain induction in vascular endothelial cells on human and mouse atheromas and its roles in ve-cadherin disorganization and atherosclerosis. Circulation. 2011; 124:2522–2532. [PubMed: 22064597]
6. Cybulsky MI, Gimbrone MA Jr. Endothelial expression of a mononuclear leukocyte adhesion molecule during atherogenesis. Science. 1991; 251:788–791. [PubMed: 1990440]
7. Davies MJ, Gordon JL, Gearing AJ, Pigott R, Woolf N, Katz D, Kyriakopoulos A. The expression of the adhesion molecules icam-1, vcam-1, pecam, and e-selectin in human atherosclerosis. J Pathol. 1993; 171:223–229. [PubMed: 7506307]
8. Kelly KA, Nahrendorf M, Yu AM, Reynolds F, Weissleder R. In vivo phage display selection yields atherosclerotic plaque targeted peptides for imaging. Mol Imaging Biol. 2006; 8:201–207. [PubMed: 16791746]
9. Broisat A, Riou LM, Ardisson V, Boturyn D, Dumy P, Fagret D, Ghezzi C. Molecular imaging of vascular cell adhesion molecule-1 expression in experimental atherosclerotic plaques with radiolabelled b2702-p. Eur J Nucl Med Mol Imaging. 2007; 34:830–840. [PubMed: 17219135]
10. Kaufmann BA, Sanders JM, Davis C, Xie A, Aldred P, Sarembock IJ, Lindner JR. Molecular imaging of inflammation in atherosclerosis with targeted ultrasound detection of vascular cell adhesion molecule-1. Circulation. 2007; 116:276–284. [PubMed: 17592078]
11. Ferrante EA, Pickard JE, Rychak J, Klibanov A, Ley K. Dual targeting improves microbubble contrast agent adhesion to vcam-1 and p-selectin under flow. J Control Release. 2009; 140:100–107. [PubMed: 19666063]
12. Southworth R, Kaneda M, Chen J, Zhang L, Zhang H, Yang X, Razavi R, Lanza G, Wickline SA. Renal vascular inflammation induced by western diet in apoe-null mice quantified by (19)f nmr of vcam-1 targeted nanobeacons. Nanomedicine. 2009; 5:359–367. [PubMed: 19523428]
13. Nahrendorf M, Jaffer FA, Kelly KA, Sosnovik DE, Aikawa E, Libby P, Weissleder R. Noninvasive vascular cell adhesion molecule-1 imaging identifies inflammatory activation of cells in atherosclerosis. Circulation. 2006; 114:1504–1511. [PubMed: 17000904]
14. Nahrendorf M, Keliher E, Panizzi P, Zhang H, Hembrador S, Figueiredo JL, Aikawa E, Kelly K, Libby P, Weissleder R. 18f-4v for pet-ct imaging of vcam-1 expression in atherosclerosis. JACC Cardiovasc Imaging. 2009; 2:1213–1222. [PubMed: 19833312]
15. Kaufmann BA, Carr CL, Belcik JT, Xie A, Yue Q, Chadderdon S, Caplan ES, Khangura J, Bullens S, Bunting S, Lindner JR. Molecular imaging of the initial inflammatory response in atherosclerosis: Implications for early detection of disease. Arterioscler Thromb Vasc Biol. 2010; 30:54–59. [PubMed: 19834105]
16. McAteer MA, Akhtar AM, von Zur Muhlen C, Choudhury RP. An approach to molecular imaging of atherosclerosis, thrombosis, and vascular inflammation using microparticles of iron oxide. Atherosclerosis. 2010; 209:18–27. [PubMed: 19883911]
17. McAteer MA, Schneider JE, Ali ZA, Warrick N, Bursill CA, von zur Muhlen C, Greaves DR, Neubauer S, Channon KM, Choudhury RP. Magnetic resonance imaging of endothelial adhesion molecules in mouse atherosclerosis using dual-targeted microparticles of iron oxide. Arterioscler Thromb Vasc Biol. 2008; 28:77–83. [PubMed: 17962629]
18. Villanueva FS, Jankowski RJ, Klibanov S, Pina ML, Alber SM, Watkins SC, Brandenburger GH, Wagner WR. Microbubbles targeted to intercellular adhesion molecule-1 bind to activated coronary artery endothelial cells. Circulation. 1998; 98:1–5. [PubMed: 9665051]
19. Demos SM, Alkan-Onyuksel H, Kane BJ, Ramani K, Nagaraj A, Greene R, Klegerman M, McPherson DD. In vivo targeting of acoustically reflective liposomes for intravascular and transvascular ultrasonic enhancement. J Am Coll Cardiol. 1999; 33:867–875. [PubMed: 10080492]
20. Jefferson A, Wijesurendra RS, McAteer MA, Digby JE, Douglas G, Bannister T, Perez-Balderas F, Bagi Z, Lindsay AC, Choudhury RP. Molecular imaging with optical coherence tomography using ligand-conjugated microparticles that detect activated endothelial cells: Rational design through target quantification. Atherosclerosis. 2011; 219:579–587. [PubMed: 21872249]

21. Robbins CS, Chudnovskiy A, Rauch PJ, Figueiredo JL, Iwamoto Y, Gorbatov R, Etzrodt M, Weber GF, Ueno T, van Rooijen N, Mulligan-Kehoe MJ, Libby P, Nahrendorf M, Pittet MJ, Weissleder R, Swirski FK. Extramedullary hematopoiesis generates ly-6chigh monocytes that infiltrate atherosclerotic lesions. Circulation. 2012; 125:364–374. [PubMed: 22144566]
22. Ramirez R, Carracedo J, Merino A, Soriano S, Ojeda R, Alvarez-Lara MA, Martin-Malo A, Aljama P. Cd14+cd16+ monocytes from chronic kidney disease patients exhibit increased adhesion ability to endothelial cells. Contrib Nephrol. 2011; 171:57–61. [PubMed: 21625090]
23. Imanishi T, Ikejima H, Tsujioka H, Kuroi A, Ishibashi K, Komukai K, Tanimoto T, Ino Y, Takeshita T, Akasaka T. Association of monocyte subset counts with coronary fibrous cap thickness in patients with unstable angina pectoris. Atherosclerosis. 2010; 212:628–635. [PubMed: 20615506]
24. Subimerb C, Pinlaor S, Lulitanond V, Khuntikeo N, Okada S, McGrath MS, Wongkham S. Circulating cd14(+) cd16(+) monocyte levels predict tissue invasive character of cholangiocarcinoma. Clin Exp Immunol. 2010; 161:471–479. [PubMed: 20636398]
25. Schlitt A, Heine GH, Blankenberg S, Espinola-Klein C, Dopheide JF, Bickel C, Lackner KJ, Iz M, Meyer J, Darius H, Rupprecht HJ. Cd14+cd16+ monocytes in coronary artery disease and their relationship to serum tnf-alpha levels. Thromb Haemost. 2004; 92:419–424. [PubMed: 15269840]
26. Paulson KE, Zhu SN, Chen M, Nurmohamed S, Jongstra-Bilen J, Cybulsky MI. Resident intimal dendritic cells accumulate lipid and contribute to the initiation of atherosclerosis. Circ Res. 2010; 106:383–390. [PubMed: 19893012]
27. Ruehm SG, Corot C, Vogt P, Kolb S, Debatin JF. Magnetic resonance imaging of atherosclerotic plaque with ultrasmall superparamagnetic particles of iron oxide in hyperlipidemic rabbits. Circulation. 2001; 103:415–422. [PubMed: 11157694]
28. Korosoglou G, Weiss RG, Kedziorek DA, Walczak P, Gilson WD, Schar M, Sosnovik DE, Kraitchman DL, Boston RC, Bulte JW, Weissleder R, Stuber M. Noninvasive detection of macrophage-rich atherosclerotic plaque in hyperlipidemic rabbits using “positive contrast” magnetic resonance imaging. J Am Coll Cardiol. 2008; 52:483–491. [PubMed: 18672170]
29. Morishige K, Kacher DF, Libby P, Josephson L, Ganz P, Weissleder R, Aikawa M. High-resolution magnetic resonance imaging enhanced with superparamagnetic nanoparticles measures macrophage burden in atherosclerosis. Circulation. 2010; 122:1707–1715. [PubMed: 20937980]
30. Settles M, Etzrodt M, Kosanke K, Schiemann M, Zimmermann A, Meier R, Braren R, Huber A, Rummeny EJ, Weissleder R, Swirski FK, Wildgruber M. Different capacity of monocyte subsets to phagocytose iron-oxide nanoparticles. PLoS One. 2011; 6:e25197. [PubMed: 21984904]
31. Tang TY, Howarth SP, Miller SR, Graves MJ, Patterson AJ, JMUK-I, Li ZY, Walsh SR, Brown AP, Kirkpatrick PJ, Warburton EA, Hayes PD, Varty K, Boyle JR, Gaunt ME, Zalewski A, Gillard JH. The atheroma (atorvastatin therapy: Effects on reduction of macrophage activity) study. Evaluation using ultrasmall superparamagnetic iron oxide-enhanced magnetic resonance imaging in carotid disease. J Am Coll Cardiol. 2009; 53:2039–2050. [PubMed: 19477353]
32. Nahrendorf M, Zhang H, Hembrador S, Panizzi P, Sosnovik DE, Aikawa E, Libby P, Swirski FK, Weissleder R. Nanoparticle pet-ct imaging of macrophages in inflammatory atherosclerosis. Circulation. 2008; 117:379–387. [PubMed: 18158358]
33. Tassa C, Shaw SY, Weissleder R. Dextran-coated iron oxide nanoparticles: A versatile platform for targeted molecular imaging, molecular diagnostics, and therapy. Acc Chem Res. 2011; 44:842–852. [PubMed: 21661727]
34. Hyafil F, Cornily JC, Feig JE, Gordon R, Vucic E, Amirbekian V, Fisher EA, Fuster V, Feldman LJ, Fayad ZA. Noninvasive detection of macrophages using a nanoparticulate contrast agent for computed tomography. Nat Med. 2007; 13:636–641. [PubMed: 17417649]
35. Seimon TA, Nadolski MJ, Liao X, Magallon J, Nguyen M, Feric NT, Koschinsky ML, Harkewicz R, Witztum JL, Tsimikas S, Golenbock D, Moore KJ, Tabas I. Atherogenic lipids and lipoproteins trigger cd36-tlr2-dependent apoptosis in macrophages undergoing endoplasmic reticulum stress. Cell Metab. 2010; 12:467–482. [PubMed: 21035758]
36. Miller YI, Choi SH, Fang L, Tsimikas S. Lipoprotein modification and macrophage uptake: Role of pathologic cholesterol transport in atherogenesis. Subcell Biochem. 2010; 51:229–251. [PubMed: 20213546]

37. Libby P. Lesion versus lumen. Nat Med. 1995; 1:17–18. [PubMed: 7584941]
38. Falk E, Shah PK, Fuster V. Coronary plaque disruption. Circulation. 1995; 92:657–671. [PubMed: 7634481]
39. Lees AM, Lees RS, Schoen FJ, Isaacsohn JL, Fischman AJ, McKusick KA, Strauss HW. Imaging human atherosclerosis with 99mtc-labeled low density lipoproteins. Arteriosclerosis. 1988; 8:461–470. [PubMed: 3190553]
40. Frias JC, Lipinski MJ, Lipinski SE, Albelda MT. Modified lipoproteins as contrast agents for imaging of atherosclerosis. Contrast Media Mol Imaging. 2007; 2:16–23. [PubMed: 17318917]
41. Sinzinger H, Bergmann H, Kaliman J, Angelberger P. Imaging of human atherosclerotic lesions using 123i-low-density lipoprotein. Eur J Nucl Med. 1986; 12:291–292. [PubMed: 3780773]
42. Amirbekian V, Lipinski MJ, Briley-Saebo KC, Amirbekian S, Aguinaldo JG, Weinreb DB, Vucic E, Frias JC, Hyafil F, Mani V, Fisher EA, Fayad ZA. Detecting and assessing macrophages in vivo to evaluate atherosclerosis noninvasively using molecular mri. Proc Natl Acad Sci U S A. 2007; 104:961–966. [PubMed: 17215360]
43. Daub K, Langer H, Seizer P, Stellos K, May AE, Goyal P, Bigalke B, Schonberger T, Geisler T, Siegel-Axel D, Oostendorp RA, Lindemann S, Gawaz M. Platelets induce differentiation of human cd34+ progenitor cells into foam cells and endothelial cells. FASEB J. 2006; 20:2559–2561. [PubMed: 17077283]
44. Ishino S, Mukai T, Kuge Y, Kume N, Ogawa M, Takai N, Kamihashi J, Shiomi M, Minami M, Kita T, Saji H. Targeting of lectinlike oxidized low-density lipoprotein receptor 1 (lox-1) with 99mtc-labeled anti-lox-1 antibody: Potential agent for imaging of vulnerable plaque. J Nucl Med. 2008; 49:1677–1685. [PubMed: 18794262]
45. Li D, Patel AR, Klibanov AL, Kramer CM, Ruiz M, Kang BY, Mehta JL, Beller GA, Glover DK, Meyer CH. Molecular imaging of atherosclerotic plaques targeted to oxidized ldl receptor lox-1 by spect/ct and magnetic resonance. Circ Cardiovasc Imaging. 2010; 3:464–472. [PubMed: 20442371]
46. Anderson DR, Duryee MJ, Anchan RK, Garvin RP, Johnston MD, Porter TR, Thiele GM, Klassen LW. Albumin-based microbubbles bind up-regulated scavenger receptors following vascular injury. J Biol Chem. 2010; 285:40645–40653. [PubMed: 20966069]
47. Vinegoni C, Botnaru I, Aikawa E, Calfon MA, Iwamoto Y, Folco EJ, Ntziachristos V, Weissleder R, Libby P, Jaffer FA. Indocyanine green enables near-infrared fluorescence imaging of lipid-rich, inflamed atherosclerotic plaques. Sci Transl Med. 2011; 3:84ra45.
48. Pedersen SF, Graebe M, Fisker Hag AM, Hojgaard L, Sillesen H, Kjaer A. Gene expression and 18fdg uptake in atherosclerotic carotid plaques. Nucl Med Commun. 2010; 31:423–429. [PubMed: 20145577]
49. Dweck MR, Jones C, Joshi NV, Fletcher AM, Richardson H, White A, Marsden M, Pessotto R, Clark JC, Wallace WA, Salter DM, McKillop G, van Beek EJ, Boon NA, Rudd JH, Newby DE. Assessment of valvular calcification and inflammation by positron emission tomography in patients with aortic stenosis. Circulation. 2012; 125:76–86. [PubMed: 22090163]
50. Fayad ZA, Mani V, Woodward M, Kallend D, Abt M, Burgess T, Fuster V, Ballantyne CM, Stein EA, Tardif JC, Rudd JH, Farkouh ME, Tawakol A. Safety and efficacy of dalcetrapib on atherosclerotic disease using novel non-invasive multimodality imaging (dal-plaque): A randomised clinical trial. Lancet. 2011; 378:1547–1559. [PubMed: 21908036]
51. Tahara N, Kai H, Ishibashi M, Nakaura H, Kaida H, Baba K, Hayabuchi N, Imaizumi T. Simvastatin attenuates plaque inflammation: Evaluation by fluorodeoxyglucose positron emission tomography. J Am Coll Cardiol. 2006; 48:1825–1831. [PubMed: 17084257]
52. Lee SJ, On YK, Lee EJ, Choi JY, Kim BT, Lee KH. Reversal of vascular 18f-fdg uptake with plasma high-density lipoprotein elevation by atherogenic risk reduction. J Nucl Med. 2008; 49:1277–1282. [PubMed: 18632820]
53. Tawakol A, Migrino RQ, Hoffmann U, Abbara S, Houser S, Gewirtz H, Muller JE, Brady TJ, Fischman AJ. Noninvasive in vivo measurement of vascular inflammation with f-18 fluorodeoxyglucose positron emission tomography. J Nucl Cardiol. 2005; 12:294–301. [PubMed: 15944534]

54. Folco EJ, Sheikine Y, Rocha VZ, Christen T, Shvartz E, Sukhova GK, Di Carli MF, Libby P. Hypoxia but not inflammation augments glucose uptake in human macrophages: Implications for imaging atherosclerosis with 18fluorine-labeled 2-deoxy-d-glucose positron emission tomography. J Am Coll Cardiol. 2011; 58:603–614. [PubMed: 21798423]
55. Ogawa M, Nakamura S, Saito Y, Kosugi M, Magata Y. What can be seen by 18f-fdg pet in atherosclerosis imaging? The effect of foam cell formation on 18f-fdg uptake to macrophages in vitro. J Nucl Med. 2012; 53:55–58. [PubMed: 22128324]
56. Rogers IS, Nasir K, Figueroa AL, Cury RC, Hoffmann U, Vermylen DA, Brady TJ, Tawakol A. Feasibility of fdg imaging of the coronary arteries: Comparison between acute coronary syndrome and stable angina. JACC Cardiovasc Imaging. 2010; 3:388–397. [PubMed: 20394901]
57. Matter CM, Wyss MT, Meier P, Spath N, von Lukowicz T, Lohmann C, Weber B, Ramirez de Molina A, Lacal JC, Ametamey SM, von Schulthess GK, Luscher TF, Kaufmann PA, Buck A. 18f-choline images murine atherosclerotic plaques ex vivo. Arterioscler Thromb Vasc Biol. 2006; 26:584–589. [PubMed: 16357314]
58. Gaemperli O, Shalhoub J, Owen DR, Lamare F, Johansson S, Fouladi N, Davies AH, Rimoldi OE, Camici PG. Imaging intraplaque inflammation in carotid atherosclerosis with 11c-pk11195 positron emission tomography/computed tomography. Eur Heart J. 2011
59. Devries-Seimon T, Li Y, Yao PM, Stone E, Wang Y, Davis RJ, Flavell R, Tabas I. Cholesterol-induced macrophage apoptosis requires er stress pathways and engagement of the type a scavenger receptor. J Cell Biol. 2005; 171:61–73. [PubMed: 16203857]
60. Laufer EM, Winkens HM, Corsten MF, Reutelingsperger CP, Narula J, Hofstra L. Pet and spect imaging of apoptosis in vulnerable atherosclerotic plaques with radiolabeled annexin a5. Q J Nucl Med Mol Imaging. 2009; 53:26–34. [PubMed: 19182725]
61. Johnson LL, Schofield L, Donahay T, Narula N, Narula J. 99mtc-annexin v imaging for in vivo detection of atherosclerotic lesions in porcine coronary arteries. J Nucl Med. 2005; 46:1186–1193. [PubMed: 16000288]
62. Ishino S, Kuge Y, Takai N, Tamaki N, Strauss HW, Blankenberg FG, Shiomi M, Saji H. 99mtc-annexin a5 for noninvasive characterization of atherosclerotic lesions: Imaging and histological studies in myocardial infarction-prone watanabe heritable hyperlipidemic rabbits. Eur J Nucl Med Mol Imaging. 2007; 34:889–899. [PubMed: 17216472]
63. Hofstra L, Liem IH, Dumont EA, Boersma HH, van Heerde WL, Doevendans PA, De Muinck E, Wellens HJ, Kemerink GJ, Reutelingsperger CP, Heidendal GA. Visualisation of cell death in vivo in patients with acute myocardial infarction. Lancet. 2000; 356:209–212. [PubMed: 10963199]
64. Kietselaer BL, Reutelingsperger CP, Heidendal GA, Daemen MJ, Mess WH, Hofstra L, Narula J. Noninvasive detection of plaque instability with use of radiolabeled annexin a5 in patients with carotid-artery atherosclerosis. N Engl J Med. 2004; 350:1472–1473. [PubMed: 15070807]
65. Sosnovik DE, Garanger E, Aikawa E, Nahrendorf M, Figuiredo JL, Dai G, Reynolds F, Rosenzweig A, Weissleder R, Josephson L. Molecular mri of cardiomyocyte apoptosis with simultaneous delayed-enhancement mri distinguishes apoptotic and necrotic myocytes in vivo: Potential for midmyocardial salvage in acute ischemia. Circ Cardiovasc Imaging. 2009; 2:460–467. [PubMed: 19920044]
66. van Tilborg GA, Mulder WJ, Deckers N, Storm G, Reutelingsperger CP, Strijkers GJ, Nicolay K. Annexin a5-functionalized bimodal lipid-based contrast agents for the detection of apoptosis. Bioconjug Chem. 2006; 17:741–749. [PubMed: 16704213]
67. Torzewski M, Shaw PX, Han KR, Shortal B, Lackner KJ, Witztum JL, Palinski W, Tsimikas S. Reduced in vivo aortic uptake of radiolabeled oxidation-specific antibodies reflects changes in plaque composition consistent with plaque stabilization. Arterioscler Thromb Vasc Biol. 2004; 24:2307–2312. [PubMed: 15528482]
68. Briley-Saebo KC, Cho YS, Tsimikas S. Imaging of oxidation-specific epitopes in atherosclerosis and macrophage-rich vulnerable plaques. Curr Cardiovasc Imaging Rep. 2011; 4:4–16. [PubMed: 21297859]
69. Nahrendorf M, Sosnovik D, Chen JW, Panizzi P, Figueiredo JL, Aikawa E, Libby P, Swirski FK, Weissleder R. Activatable magnetic resonance imaging agent reports myeloperoxidase activity in healing infarcts and noninvasively detects the antiinflammatory effects of atorvastatin on ischemia-reperfusion injury. Circulation. 2008; 117:1153–1160. [PubMed: 18268141]

70. Panizzi P, Nahrendorf M, Wildgruber M, Waterman P, Figueiredo JL, Aikawa E, McCarthy J, Weissleder R, Hilderbrand SA. Oxazine conjugated nanoparticle detects in vivo hypochlorous acid and peroxynitrite generation. J Am Chem Soc. 2009; 131:15739–15744. [PubMed: 19817443]
71. Moreno PR, Purushothaman KR, Fuster V, Echeverri D, Truszczynska H, Sharma SK, Badimon JJ, O'Connor WN. Plaque neovascularization is increased in ruptured atherosclerotic lesions of human aorta: Implications for plaque vulnerability. Circulation. 2004; 110:2032–2038. [PubMed: 15451780]
72. Lal H, Verma SK, Foster DM, Golden HB, Reneau JC, Watson LE, Singh H, Dostal DE. Integrins and proximal signaling mechanisms in cardiovascular disease. Front Biosci. 2009; 14:2307–2334. [PubMed: 19273203]
73. Winter PM, Morawski AM, Caruthers SD, Fuhrhop RW, Zhang H, Williams TA, Allen JS, Lacy EK, Robertson JD, Lanza GM, Wickline SA. Molecular imaging of angiogenesis in early-stage atherosclerosis with alpha(v)beta3-integrin-targeted nanoparticles. Circulation. 2003; 108:2270–2274. [PubMed: 14557370]
74. Burtea C, Laurent S, Murariu O, Rattat D, Toubeau G, Verbruggen A, Vansthertem D, Vander Elst L, Muller RN. Molecular imaging of alpha v beta3 integrin expression in atherosclerotic plaques with a mimetic of rgd peptide grafted to gd-dtpa. Cardiovasc Res. 2008; 78:148–157. [PubMed: 18174291]
75. Winter PM, Neubauer AM, Caruthers SD, Harris TD, Robertson JD, Williams TA, Schmieder AH, Hu G, Allen JS, Lacy EK, Zhang H, Wickline SA, Lanza GM. Endothelial alpha(v)beta3 integrin-targeted fumagillin nanoparticles inhibit angiogenesis in atherosclerosis. Arterioscler Thromb Vasc Biol. 2006; 26:2103–2109. [PubMed: 16825592]
76. Winter PM, Caruthers SD, Zhang H, Williams TA, Wickline SA, Lanza GM. Antiangiogenic synergism of integrin-targeted fumagillin nanoparticles and atorvastatin in atherosclerosis. JACC Cardiovasc Imaging. 2008; 1:624–634. [PubMed: 19356492]
77. Laitinen I, Saraste A, Weidl E, Poethko T, Weber AW, Nekolla SG, Leppanen P, Yla-Herttuala S, Holzlwimmer G, Walch A, Esposito I, Wester HJ, Knuuti J, Schwaiger M. Evaluation of alphavbeta3 integrin-targeted positron emission tomography tracer 18f-galacto-rgd for imaging of vascular inflammation in atherosclerotic mice. Circ Cardiovasc Imaging. 2009; 2:331–338. [PubMed: 19808614]
78. Partovi S, Loebe M, Aschwanden M, Baldi T, Jager KA, Feinstein SB, Staub D. Contrast-enhanced ultrasound for assessing carotid atherosclerotic plaque lesions. AJR Am J Roentgenol. 2012; 198:W13–19. [PubMed: 22194509]
79. Heroux J, Gharib AM, Danthi NS, Cecchini S, Ohayon J, Pettigrew RI. High-affinity alphavbeta3 integrin targeted optical probe as a new imaging biomarker for early atherosclerosis: Initial studies in watanabe rabbits. Mol Imaging Biol. 2010; 12:2–8. [PubMed: 19898904]
80. O'Brien KD, McDonald TO, Chait A, Allen MD, Alpers CE. Neovascular expression of e-selectin, intercellular adhesion molecule-1, and vascular cell adhesion molecule-1 in human atherosclerosis and their relation to intimal leukocyte content. Circulation. 1996; 93:672–682. [PubMed: 8640995]
81. Wallis de Vries BM, Hillebrands JL, van Dam GM, Tio RA, de Jong JS, Slart RH, Zeebregts CJ. Images in cardiovascular medicine. Multispectral near-infrared fluorescence molecular imaging of matrix metalloproteinases in a human carotid plaque using a matrix-degrading metalloproteinase-sensitive activatable fluorescent probe. Circulation. 2009; 119:e534–536. [PubMed: 19470893]
82. Razansky D, Harlaar NJ, Hillebrands JL, Taruttis A, Herzog E, Zeebregts CJ, van Dam GM, Ntziachristos V. Multispectral optoacoustic tomography of matrix metalloproteinase activity in vulnerable human carotid plaques. Mol Imaging Biol. 2011
83. Deguchi JO, Aikawa M, Tung CH, Aikawa E, Kim DE, Ntziachristos V, Weissleder R, Libby P. Inflammation in atherosclerosis: Visualizing matrix metalloproteinase action in macrophages in vivo. Circulation. 2006; 114:55–62. [PubMed: 16801460]
84. Quillard T, Tesmenitsky Y, Croce K, Travers R, Shvartz E, Koskinas KC, Sukhova GK, Aikawa E, Aikawa M, Libby P. Selective inhibition of matrix metalloproteinase-13 increases collagen content of established mouse atherosclerosis. Arterioscler Thromb Vasc Biol. 2011; 31:2464–2472. [PubMed: 21903941]
85. Chang K, Francis SA, Aikawa E, Figueiredo JL, Kohler RH, McCarthy JR, Weissleder R, Plutzky J, Jaffer FA. Pioglitazone suppresses inflammation in vivo in murine carotid atherosclerosis:

Novel detection by dual-target fluorescence molecular imaging. Arterioscler Thromb Vasc Biol. 2010; 30:1933–1939. [PubMed: 20689078]

86. Kim DE, Kim JY, Schellingerhout D, Shon SM, Jeong SW, Kim EJ, Kim WK. Molecular imaging of cathepsin b proteolytic enzyme activity reflects the inflammatory component of atherosclerotic pathology and can quantitatively demonstrate the antiatherosclerotic therapeutic effects of atorvastatin and glucosamine. Mol Imaging. 2009; 8:291–301. [PubMed: 19796606]
87. Jaffer FA, Kim DE, Quinti L, Tung CH, Aikawa E, Pande AN, Kohler RH, Shi GP, Libby P, Weissleder R. Optical visualization of cathepsin k activity in atherosclerosis with a novel, protease-activatable fluorescence sensor. Circulation. 2007; 115:2292–2298. [PubMed: 17420353]
88. Aikawa E, Aikawa M, Libby P, Figueiredo JL, Rusanescu G, Iwamoto Y, Fukuda D, Kohler RH, Shi GP, Jaffer FA, Weissleder R. Arterial and aortic valve calcification abolished by elastolytic cathepsin s deficiency in chronic renal disease. Circulation. 2009; 119:1785–1794. [PubMed: 19307473]
89. Jaffer FA, Vinegoni C, John MC, Aikawa E, Gold HK, Finn AV, Ntziachristos V, Libby P, Weissleder R. Real-time catheter molecular sensing of inflammation in proteolytically active atherosclerosis. Circulation. 2008; 118:1802–1809. [PubMed: 18852366]
90. Olson ES, Jiang T, Aguilera TA, Nguyen QT, Ellies LG, Scadeng M, Tsien RY. Activatable cell penetrating peptides linked to nanoparticles as dual probes for in vivo fluorescence and mr imaging of proteases. Proc Natl Acad Sci U S A. 2010; 107:4311–4316. [PubMed: 20160077]
91. Liu CH, You Z, Liu CM, Kim YR, Whalen MJ, Rosen BR, Liu PK. Diffusion-weighted magnetic resonance imaging reversal by gene knockdown of matrix metalloproteinase-9 activities in live animal brains. J Neurosci. 2009; 29:3508–3517. [PubMed: 19295156]
92. Watkins GA, Jones EF, Scott Shell M, VanBrocklin HF, Pan MH, Hanrahan SM, Feng JJ, He J, Sounni NE, Dill KA, Contag CH, Coussens LM, Franc BL. Development of an optimized activatable mmp-14 targeted spect imaging probe. Bioorg Med Chem. 2009; 17:653–659. [PubMed: 19109023]
93. Amirbekian V, Aguinaldo JG, Amirbekian S, Hyafil F, Vucic E, Sirol M, Weinreb DB, Le Greneur S, Lancelot E, Corot C, Fisher EA, Galis ZS, Fayad ZA. Atherosclerosis and matrix metalloproteinases: Experimental molecular mr imaging in vivo. Radiology. 2009; 251:429–438. [PubMed: 19224894]
94. Sprague JE, Li WP, Liang K, Achilefu S, Anderson CJ. In vitro and in vivo investigation of matrix metalloproteinase expression in metastatic tumor models. Nucl Med Biol. 2006; 33:227–237. [PubMed: 16546677]
95. Zhu L, Xie J, Swierczewska M, Zhang F, Quan Q, Ma Y, Fang X, Kim K, Lee S, Chen X. Real-time video imaging of protease expression in vivo. Theranostics. 2011; 1:18–27. [PubMed: 21461134]
96. Haider N, Hartung D, Fujimoto S, Petrov A, Kolodgie FD, Virmani R, Ohshima S, Liu H, Zhou J, Fujimoto A, Tahara A, Hofstra L, Narula N, Reutelingsperger C, Narula J. Dual molecular imaging for targeting metalloproteinase activity and apoptosis in atherosclerosis: Molecular imaging facilitates understanding of pathogenesis. J Nucl Cardiol. 2009; 16:753–762. [PubMed: 19662466]
97. Razavian M, Tavakoli S, Zhang J, Nie L, Dobrucki LW, Sinusas AJ, Azure M, Robinson S, Sadeghi MM. Atherosclerosis plaque heterogeneity and response to therapy detected by in vivo molecular imaging of matrix metalloproteinase activation. J Nucl Med. 2011; 52:1795–1802. [PubMed: 21969358]
98. Klink A, Heynens J, Herranz B, Lobatto ME, Arias T, Sanders HM, Strijkers GJ, Merkx M, Nicolay K, Fuster V, Tedgui A, Mallat Z, Mulder WJ, Fayad ZA. In vivo characterization of a new abdominal aortic aneurysm mouse model with conventional and molecular magnetic resonance imaging. J Am Coll Cardiol. 2011; 58:2522–2530. [PubMed: 22133853]
99. Reulen SW, Dankers PY, Bomans PH, Meijer EW, Merkx M. Collagen targeting using protein-functionalized micelles: The strength of multiple weak interactions. J Am Chem Soc. 2009; 131:7304–7312. [PubMed: 19469576]
100. Megens RT, Reitsma S, Prinzen L, oude Egbrink MG, Engels W, Leenders PJ, Brunenberg EJ, Reesink KD, Janssen BJ, ter Haar Romeny BM, Slaaf DW, van Zandvoort MA. In vivo high-

resolution structural imaging of large arteries in small rodents using two-photon laser scanning microscopy. J Biomed Opt. 2010; 15:011108. [PubMed: 20210434]

101. Sukhova GK, Schonbeck U, Rabkin E, Schoen FJ, Poole AR, Billinghurst RC, Libby P. Evidence for increased collagenolysis by interstitial collagenases-1 and -3 in vulnerable human atheromatous plaques. Circulation. 1999; 99:2503–2509. [PubMed: 10330380]
102. Newby AC. Metalloproteinase expression in monocytes and macrophages and its relationship to atherosclerotic plaque instability. Arterioscler Thromb Vasc Biol. 2008; 28:2108–2114. [PubMed: 18772495]
103. Jacobin-Valat MJ, Deramchia K, Mornet S, Hagemeyer CE, Bonetto S, Robert R, Biran M, Massot P, Miraux S, Sanchez S, Bouzier-Sore AK, Franconi JM, Duguet E, Clofent-Sanchez G. Mri of inducible p-selectin expression in human activated platelets involved in the early stages of atherosclerosis. NMR Biomed. 2010
104. Rouzet F, Bachelet-Violette L, Alsac JM, Suzuki M, Meulemans A, Louedec L, Petiet A, Jandrot-Perrus M, Chaubet F, Michel JB, Le Guludec D, Letourneur D. Radiolabeled fucoidan as a p-selectin targeting agent for in vivo imaging of platelet-rich thrombus and endothelial activation. J Nucl Med. 2011; 52:1433–1440. [PubMed: 21849401]
105. Duerschmied D, Meiner M, Peter K, Neudorfer I, Roming F, Zirlik A, Bode C, von Elverfeldt D, von Zur Muhlen C. Molecular magnetic resonance imaging allows the detection of activated platelets in a new mouse model of coronary artery thrombosis. Invest Radiol. 2011; 46:618–623. [PubMed: 21577120]
106. von zur Muhlen C, Peter K, Ali ZA, Schneider JE, McAteer MA, Neubauer S, Channon KM, Bode C, Choudhury RP. Visualization of activated platelets by targeted magnetic resonance imaging utilizing conformation-specific antibodies against glycoprotein iib/iiia. J Vasc Res. 2009; 46:6–14. [PubMed: 18515970]
107. von zur Muhlen C, von Elverfeldt D, Moeller JA, Choudhury RP, Paul D, Hagemeyer CE, Olschewski M, Becker A, Neudorfer I, Bassler N, Schwarz M, Bode C, Peter K. Magnetic resonance imaging contrast agent targeted toward activated platelets allows in vivo detection of thrombosis and monitoring of thrombolysis. Circulation. 2008; 118:258–267. [PubMed: 18574047]
108. Vymazal J, Spuentrup E, Cardenas-Molina G, Wiethoff AJ, Hartmann MG, Caravan P, Parsons EC Jr. Thrombus imaging with fibrin-specific gadolinium-based mr contrast agent ep-2104r: Results of a phase ii clinical study of feasibility. Invest Radiol. 2009; 44:697–704. [PubMed: 19809344]
109. Uppal R, Catana C, Ay I, Benner T, Sorensen AG, Caravan P. Bimodal thrombus imaging: Simultaneous pet/mr imaging with a fibrin-targeted dual pet/mr probe--feasibility study in rat model. Radiology. 2011; 258:812–820. [PubMed: 21177389]
110. McCarthy JR, Patel P, Botnaru I, Haghayeghi P, Weissleder R, Jaffer FA. Multimodal nanoagents for the detection of intravascular thrombi. Bioconjug Chem. 2009; 20:1251–1255. [PubMed: 19456115]
111. Jaffer FA, Tung CH, Wykrzykowska JJ, Ho NH, Houng AK, Reed GL, Weissleder R. Molecular imaging of factor xiiia activity in thrombosis using a novel, near-infrared fluorescent contrast agent that covalently links to thrombi. Circulation. 2004; 110:170–176. [PubMed: 15210587]
112. Tei L, Mazooz G, Shellef Y, Avni R, Vandoorne K, Barge A, Kalchenko V, Dewhirst MW, Chaabane L, Miragoli L, Longo D, Neeman M, Aime S. Novel mri and fluorescent probes responsive to the factor xiii transglutaminase activity. Contrast Media Mol Imaging. 2010; 5:213–222. [PubMed: 20812289]
113. Miserus RJ, Herias MV, Prinzen L, Lobbes MB, Van Suylen RJ, Dirksen A, Hackeng TM, Heemskerk JW, van Engelshoven JM, Daemen MJ, van Zandvoort MA, Heeneman S, Kooi ME. Molecular mri of early thrombus formation using a bimodal alpha2-antiplasmin-based contrast agent. JACC Cardiovasc Imaging. 2009; 2:987–996. [PubMed: 19679287]
114. Alexopoulos N, Raggi P. Calcification in atherosclerosis. Nat Rev Cardiol. 2009; 6:681–688. [PubMed: 19786983]
115. Parikh NI, Hwang SJ, Larson MG, Cupples LA, Fox CS, Manders ES, Murabito JM, Massaro JM, Hoffmann U, O'Donnell CJ. Parental occurrence of premature cardiovascular disease

predicts increased coronary artery and abdominal aortic calcification in the framingham offspring and third generation cohorts. Circulation. 2007; 116:1473–1481. [PubMed: 17785619]

116. Folsom AR, Kronmal RA, Detrano RC, O'Leary DH, Bild DE, Bluemke DA, Budoff MJ, Liu K, Shea S, Szklo M, Tracy RP, Watson KE, Burke GL. Coronary artery calcification compared with carotid intima-media thickness in the prediction of cardiovascular disease incidence: The multi-ethnic study of atherosclerosis (mesa). Arch Intern Med. 2008; 168:1333–1339. [PubMed: 18574091]
117. O'Donnell CJ, Kavousi M, Smith AV, Kardia SL, Feitosa MF, Hwang SJ, Sun YV, Province MA, Aspelund T, Dehghan A, Hoffmann U, Bielak LF, Zhang Q, Eiriksdottir G, van Duijn CM, Fox CS, de Andrade M, Kraja AT, Sigurdsson S, Elias-Smale SE, Murabito JM, Launer LJ, van der Lugt A, Kathiresan S, Krestin GP, Herrington DM, Howard TD, Liu Y, Post W, Mitchell BD, O'Connell JR, Shen H, Shuldiner AR, Altshuler D, Elosua R, Salomaa V, Schwartz SM, Siscovick DS, Voight BF, Bis JC, Glazer NL, Psaty BM, Boerwinkle E, Heiss G, Blankenberg S, Zeller T, Wild PS, Schnabel RB, Schillert A, Ziegler A, Munzel TF, White CC, Rotter JI, Nalls M, Oudkerk M, Johnson AD, Newman AB, Uitterlinden AG, Massaro JM, Cunningham J, Harris TB, Hofman A, Peyser PA, Borecki IB, Cupples LA, Gudnason V, Witteman JC. Genome-wide association study for coronary artery calcification with follow-up in myocardial infarction. Circulation. 2011; 124:2855–2864. [PubMed: 22144573]
118. Zaheer A, Murshed M, De Grand AM, Morgan TG, Karsenty G, Frangioni JV. Optical imaging of hydroxyapatite in the calcified vasculature of transgenic animals. Arterioscler Thromb Vasc Biol. 2006; 26:1132–1136. [PubMed: 16484598]
119. Aikawa E, Nahrendorf M, Sosnovik D, Lok VM, Jaffer FA, Aikawa M, Weissleder R. Multimodality molecular imaging identifies proteolytic and osteogenic activities in early aortic valve disease. Circulation. 2007; 115:377–386. [PubMed: 17224478]
120. Aikawa E, Nahrendorf M, Figueiredo JL, Swirski FK, Shtatland T, Kohler RH, Jaffer FA, Aikawa M, Weissleder R. Osteogenesis associates with inflammation in early-stage atherosclerosis evaluated by molecular imaging in vivo. Circulation. 2007; 116:2841–2850. [PubMed: 18040026]
121. Hjortnaes J, Butcher J, Figueiredo JL, Riccio M, Kohler RH, Kozloff KM, Weissleder R, Aikawa E. Arterial and aortic valve calcification inversely correlates with osteoporotic bone remodelling: A role for inflammation. Eur Heart J. 2010; 31:1975–1984. [PubMed: 20601388]
122. Beheshti M, Saboury B, Mehta NN, Torigian DA, Werner T, Mohler E, Wilensky R, Newberg AB, Basu S, Langsteger W, Alavi A. Detection and global quantification of cardiovascular molecular calcification by fluoro18-fluoride positron emission tomography/computed tomography--a novel concept. Hell J Nucl Med. 2011; 14:114–120. [PubMed: 21761011]
123. Nasu K, Tsuchikane E, Katoh O, Tanaka N, Kimura M, Ehara M, Kinoshita Y, Matsubara T, Matsuo H, Asakura K, Asakura Y, Terashima M, Takayama T, Honye J, Hirayama A, Saito S, Suzuki T. Effect of fluvastatin on progression of coronary atherosclerotic plaque evaluated by virtual histology intravascular ultrasound. JACC Cardiovasc Interv. 2009; 2:689–696. [PubMed: 19628194]
124. Nissen SE, Nicholls SJ, Sipahi I, Libby P, Raichlen JS, Ballantyne CM, Davignon J, Erbel R, Fruchart JC, Tardif JC, Schoenhagen P, Crowe T, Cain V, Wolski K, Goormastic M, Tuzcu EM. Effect of very high-intensity statin therapy on regression of coronary atherosclerosis: The asteroid trial. JAMA. 2006; 295:1556–1565. [PubMed: 16533939]
125. Nissen SE, Tsunoda T, Tuzcu EM, Schoenhagen P, Cooper CJ, Yasin M, Eaton GM, Lauer MA, Sheldon WS, Grines CL, Halpern S, Crowe T, Blankenship JC, Kerensky R. Effect of recombinant apoa-i milano on coronary atherosclerosis in patients with acute coronary syndromes: A randomized controlled trial. JAMA. 2003; 290:2292–2300. [PubMed: 14600188]
126. Navab M, Reddy ST, Van Lenten BJ, Fogelman AM. Hdl and cardiovascular disease: Atherogenic and atheroprotective mechanisms. Nat Rev Cardiol. 2011; 8:222–232. [PubMed: 21304474]
127. Coomes E, Chan ES, Reiss AB. Methotrexate in atherogenesis and cholesterol metabolism. Cholesterol. 2011; 2011:503028. [PubMed: 21490773]
128. Fischer A, Blanche S, Le Bidois J, Bordigoni P, Garnier JL, Niaudet P, Morinet F, Le Deist F, Fischer AM, Griscelli C, et al. Anti-b-cell monoclonal antibodies in the treatment of severe b-cell

lymphoproliferative syndrome following bone marrow and organ transplantation. N Engl J Med. 1991; 324:1451–1456. [PubMed: 2023604]

129. Martin P, Furman RR, Ruan J, Elstrom R, Barrientos J, Niesvizky R, Coleman M, Leonard JP. Novel and engineered anti-b-cell monoclonal antibodies for non-hodgkin's lymphoma. Semin Hematol. 2008; 45:126–132. [PubMed: 18381108]
130. Herold KC, Pescovitz MD, McGee P, Krause-Steinrauf H, Spain LM, Bourcier K, Asare A, Liu Z, Lachin JM, Dosch HM. Increased t cell proliferative responses to islet antigens identify clinical responders to anti-cd20 monoclonal antibody (rituximab) therapy in type 1 diabetes. J Immunol. 2011; 187:1998–2005. [PubMed: 21775681]
131. Vordenbaumen S, Neuen-Jacob E, Richter J, Schneider M. Inclusion body myositis in a patient with long standing rheumatoid arthritis treated with anti-tnfalpha and rituximab. Clin Rheumatol. 2010; 29:555–558. [PubMed: 20108015]
132. Habets KL, van Puijvelde GH, van Duivenvoorde LM, van Wanrooij EJ, de Vos P, Tervaert JW, van Berkel TJ, Toes RE, Kuiper J. Vaccination using oxidized low-density lipoprotein-pulsed dendritic cells reduces atherosclerosis in ldl receptor-deficient mice. Cardiovasc Res. 2010; 85:622–630. [PubMed: 19819882]
133. Cui K, Hou G, Feng Y, Liang T, Kong F, Sun L, Wang S. The potential role of preventing atherosclerosis by induction of neonatal tolerance to vldl. Cell Immunol. 2012; 272:290–292. [PubMed: 22067889]
134. Gill EA Jr. Does statin therapy affect the progression of atherosclerosis measured by a coronary calcium score? Curr Atheroscler Rep. 2010; 12:83–87. [PubMed: 20425242]
135. Vengrenyuk Y, Cardoso L, Weinbaum S. Micro-ct based analysis of a new paradigm for vulnerable plaque rupture: Cellular microcalcifications in fibrous caps. Mol Cell Biomech. 2008; 5:37–47. [PubMed: 18524245]
136. Chiribiri A, Ishida M, Nagel E, Botnar RM. Coronary imaging with cardiovascular magnetic resonance: Current state of the art. Prog Cardiovasc Dis. 2011; 54:240–252. [PubMed: 22014491]

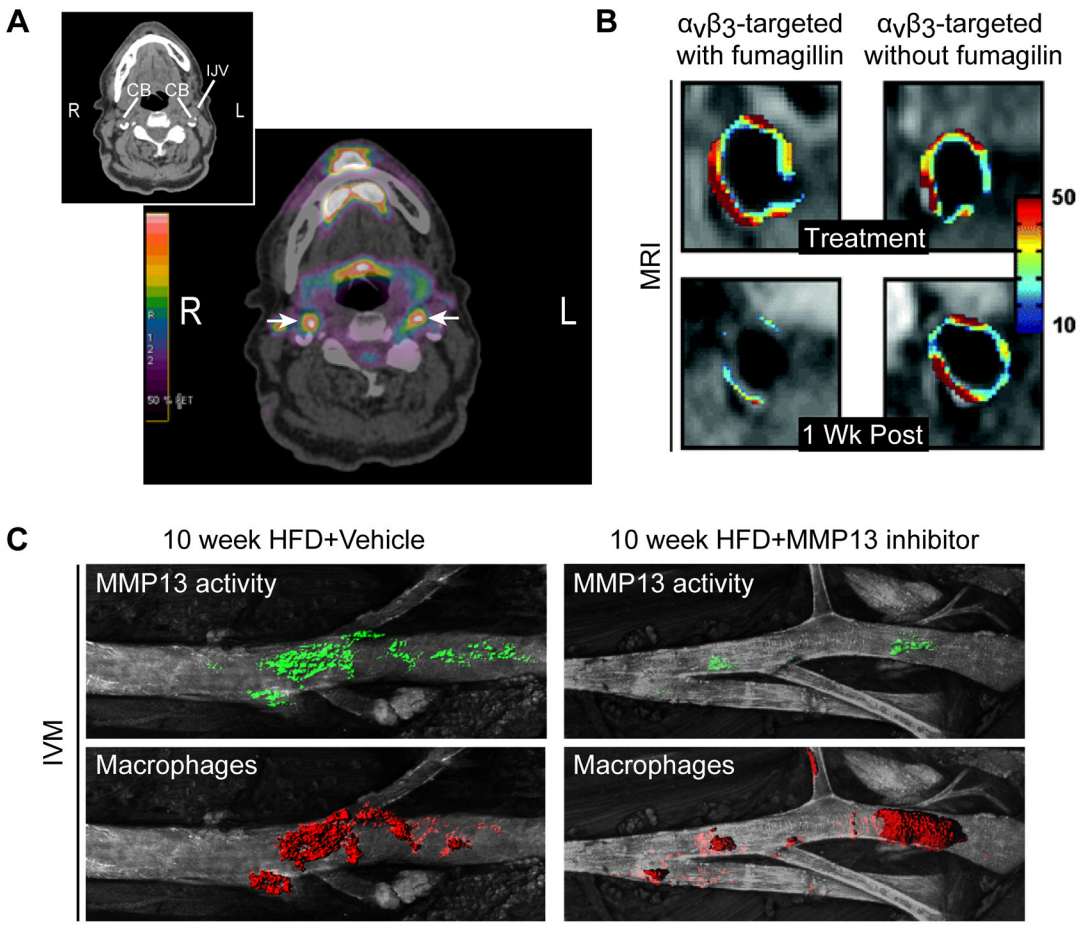

Figure 1.

A. Representative ^{18}F-FDG-PET images. The insert shows the scout CT scan, and the large frame the PET signal surimposed on the CT image. The color scale shows the level of radioactivity from low (black) to high (red). The arrows indicate FDG uptake bilaterally at the level of the carotid bifurcation (CB). (R=Right, L=Left, IJV=Internal jugular vein). Images courtesy of Marcelo F. DiCarli, Brigham and Women's Hospital. **B.** MRI of abdominal aorta from rabbits showing pseudocolored overlay of percent signal enhancement at time of treatment with integrin-targeted paramagnetic nanoparticles that incorporated fumagillin at 0 μg/kg or 30 μg/kg (top), and 1 week post-treatment (bottom). Adapted from Winter et al., *ATVB*, 2006.[75] **C.** IVM of the left carotid artery from MMP13 inhibitor–treated and untreated apoE$^{-/-}$ mice, coinjected with MMP-13 activatable probe and nanoparticles for macrophage detection. Adapted from Quillard et al., *ATVB*, 2011.[84]

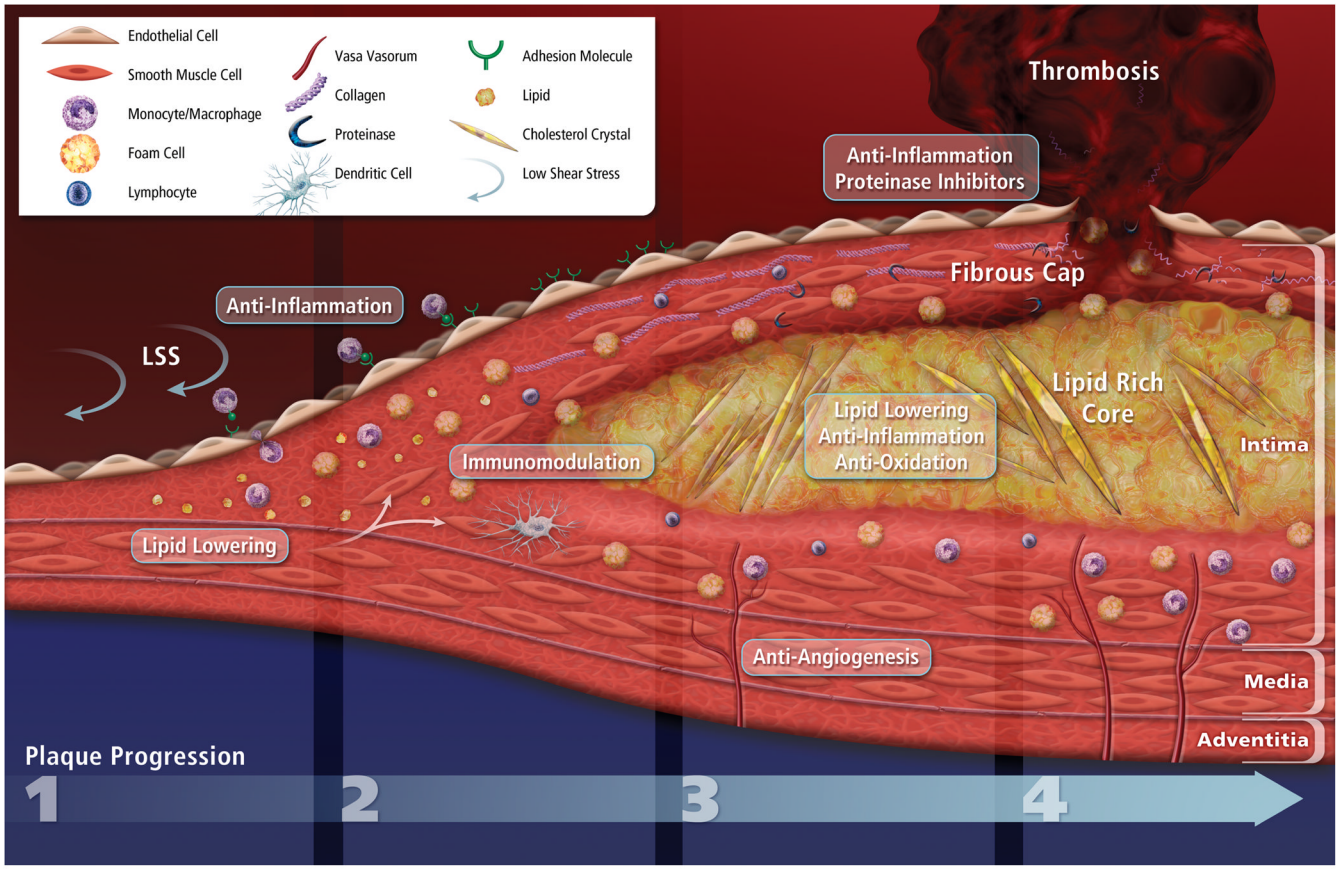

Figure 2.

Atherosclerotic plaque progression and impact on current therapeutic strategies. Atherogenesis begins with increased permeability and recruitment of inflammatory cells to the intima at sites experiencing low shear stress and disturbed flow. (1) LDL accumulates in the subendothelial matrix, and activated endothelial cells express adhesion molecules that recruit circulating leukocytes (mainly the pro-inflammatory subset monocytes at early stages). (2) Monocyte-derived macrophages uptake modified LDL particles to form foam cells. Mature foam cells release pro-inflammatory mediators that amplify local inflammation and immune-cell recruitment, reactive oxygen species, and tissue factor pro-coagulant. Foam-cell accumulation initiates the formation of a lipid-rich core, and medial SMCs proliferate and migrate within the intima. A fibrous cap composed of SMCs and ECM molecules (mainly collagen) overlies the growing lipid-rich necrotic core. (3) Limited blood perfusion of the deep layer of the lesion triggers neoangiogenic sprouting of the adventitial vasa vasorum network. In advanced lesions, the active proteinases continuously released by macrophages/foam cells digest interstitial collagen fibers, therefore reducing fibrous cap thickness and tensile strength. (4) Ultimately, physical disruption of the fibrous cap exposes the pro-thrombotic content to the blood and initiates the formation of a thrombus. Current therapeutic strategies selectively target most of the known molecular processes involved in plaque formation and development.

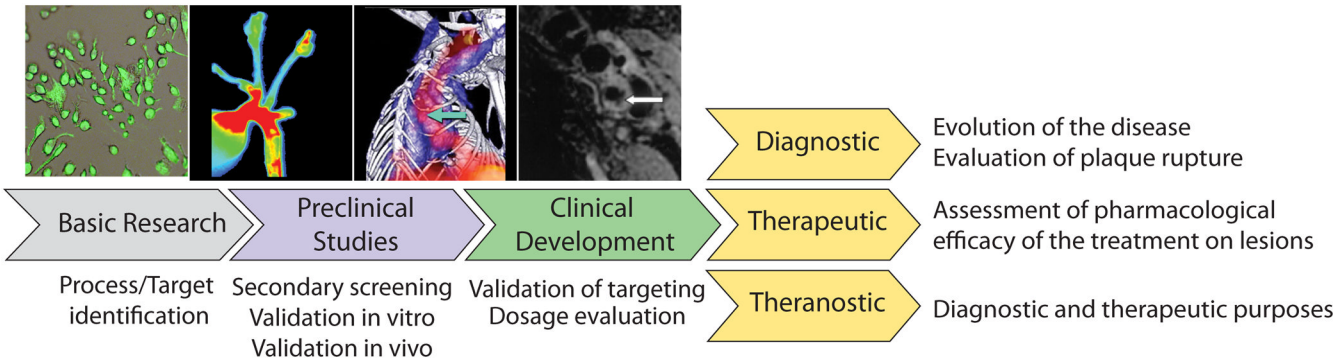

Figure 3.
Impact of molecular imaging in therapeutic and diagnostic tool development.

Table 1

Molecular targets of atherosclerotic plaques and associated imaging moieties and modalities

Molecular target	Imaging moieties	Imaging platforms	Biological process
VCAM-1	^{123}I, ^{99m}Tc, ^{18}F, SPIO, NIRF, microbubbles	PET/SPECT, MRI, optical imaging, CEU	inflammation
ICAM-1	Gd, microbubbles	MRI, CEU	inflammation
E-selectin	SPIO	MRI	inflammation
P-selectin	SPIO, Gd, microbubbles	MRI, CEU	inflammation, thrombosis
-	SPIO	MRI	phagocytic activity
-	^{64}Cu, ^{18}F-SPIO	PET/SPECT	phagocytic activity
FDG	^{18}F	PET	metabolic activity
FCH	^{18}F	PET	metabolic activity
HDL/LDL	^{123}I, ^{125}I, ^{131}I, ^{111}In, ^{99m}Tc, Gd	PET/SPECT, MRI	lipid uptake
CD68	^{124}I	PET/SPECT	lipid uptake
LOX-1	^{111}In, ^{99m}Tc, Gd	SPECT, MRI	lipid uptake
SRs	microbubbles	CEU	lipid uptake
oxidized epitopes	^{125}I, Gd, SPIO	PET/SPECT, MRI	oxidative stress
MPO	Gd	MRI	oxidative stress
phosphatidylserine	^{123}I, ^{124}I, ^{99m}Tc, Gd, SPIO	PET/SPECT, MRI	cell death
MMPs	^{123}I, ^{99m}Tc, ^{18}F, Gd, SPIO, NIRF	PET/SPECT, MRI, optical imaging	proteinase activity
cathepsins	NIRF	optical imaging	proteinase activity
collagen	Gd, NIRF	MRI, optical imaging	proteinase activity
αvβ3 integrin	^{18}F, Gd, NIRF, microbubbles	PET, MRI, optical imaging, CEU	neoangiogenesis
-	MR-contrast agent (K^{trans}), microbubbles	MRI, CEU	neoangiogenesis
Ca^{++} hydroxyapatite	^{18}F, NIRF	PET, optical imaging	osteogenesis
glycoprotein IIb/IIIa	^{99m}Tc, SPIO, NIRF, microbubbles	PET, MRI, optical imaging, CEU	thrombosis
fibrin	^{64}Cu, Gd	PET, MRI	thrombosis
factor XIII	Gd, SPIO, NIRF	MRI, optical imaging	thrombosis